JOURNAL OF MATERIALS SCIENCE 27 (1992) 6303–6310

Relationships between dopants, microstructure and the microwave dielectric properties of ZrO_2–TiO_2–SnO_2 ceramics

D. M. IDDLES, A. J. BELL*
Cookson Technology Centre, Yarnton, Oxford, UK
A. J. MOULSON
School of Materials, University of Leeds, Leeds, UK

Ceramics with compositions in the solid solution region of the ZrO_2–TiO_2–SnO_2 equilibrium diagram are finding wide application as dielectrics in filters for communications and radar systems operating at microwave frequencies. Commercially available compositions often incorporate sintering aids and dopants to reduce processing temperatures and modify the dielectric properties. However, the mechanism through which these additives influence dielectric loss is not obvious. The role of zinc oxide as a sintering aid and lanthanum and niobium as dopants, their effect upon microstructural development and their correlation with dielectric loss at microwave frequencies were investigated. For specimens of density greater than 90% theoretical, the influences of defect chemistry upon dielectric loss appear to dominate those of the microstructure. Properties close to those which might be considered intrinsic were attained through sintering for periods of up to 128 h. Doping with lanthanum is detrimental to the dielectric loss, particularly after long sintering times.

1. Introduction

The microwave frequency band is generally considered to lie in the range 0.9–300 GHz. The importance of this frequency range is recognizable in the current growth of microwave communications systems which make use of the superior information density possible at high frequencies. Direct broadcast satellite TV, hand-held (cellular) telephones and radar are examples of systems that require tight channel frequency control to maximize information density. Band pass filters, in the form of resonant cavities, are therefore common elements in such circuits.

Conventional air-cavity resonators are bulky and expensive to manufacture. However, the use of high relative permittivity, low-loss dielectrics, in the form of dielectric post resonators, coaxial resonators or as substrates for strip-line resonators, allows significant size reduction [1]. The electromagnetic theory for dielectric resonators was solved by Richtmyer [2] in 1939, who demonstrated that suitably shaped dielectric materials were capable of confining electromagnetic fields within their geometries, by internal reflection, and so act as electrical resonators.

The size reduction achieved in using dielectric resonators, compared to air cavities, is of a factor of the order of $\varepsilon_r^{1/2}$, where ε_r is the relative permittivity of the dielectric. Hence, the higher the permittivity of the material employed, the greater the size reduction. However, there are factors, other than high ε_r, which guide the choice of dielectric materials and place an approximate limit upon the achievable size reduction.

The Q of a dielectric resonator determines its selectivity and attenuation, and is directly related to the dielectric loss of the constituent material

$$Q \approx 1/\tan \delta \quad (1)$$

where $\tan \delta$ is the dielectric loss tangent. Hence, materials with low dielectric loss tangents are preferred. In addition, good temperature stability of resonant frequency is also sought. The temperature coefficient of resonant frequency,

$$\tau_f = 1/f_0(df_0/dT) \quad (2)$$

where f_0 is the resonant frequency and T is temperature, is often quoted and is related to the temperature coefficient of relative permittivity of the dielectric by

$$\tau_f = -1/2\tau_\varepsilon - \alpha \quad (3)$$

where τ_ε is the temperature coefficient of permittivity and α is the linear thermal expansion coefficient of the material. Low τ_ε is therefore also a desirable material property.

In considering a wide range of dielectric materials, it can be generally said that as ε_r increases, so do $\tan \delta$ and τ_ε, consequently the requirements for high ε_r, low

Present address: Laboratoire de Céramique, Ecole Polytechnique Federale de Lausanne, 1015 Lausanne, Switzerland.

0022–2461

tan δ and low τ_ε are to some extent incompatible. However, there is a group of materials which have been found to offer a combination of properties which are suitable for the fabrication of microwave dielectric resonators and substrates. These have properties in the range

$$10 < \varepsilon_r < 90 \quad (4a)$$

$$\tan \delta < 3 \times 10^{-4} \quad (4b)$$

$$-10 < \tau_f < 10\ \mathrm{MK}^{-1} \quad (4c)$$

Materials exhibiting properties close to these were first identified in a series of perovskite solid solutions [3, 4] formed by combining components with opposing values of τ_ε. Ca(Zr, Ti)O_3 and Sr(Zr, Ti)O_3, for example, have values of τ_f in the region of $\pm 30\ \mathrm{MK}^{-1}$, but relative permittivities are rather low for many of the intended applications. Materials such as rutile and barium tetratitanate [5] ($BaTi_4O_9$) have also been considered, but suffer from high values of τ_f, these being 400 and 50 MK^{-1}, respectively.

O'Bryan and co-workers [6–8] identified the useful dielectric properties of barium nonatitanate ($Ba_2Ti_9O_{20}$); $\varepsilon_r = 39$, $Q_{(4\,\mathrm{GHz})} = 7000$ and $\tau_f = 2\ \mathrm{MK}^{-1}$. However, this compound has been shown to have a very narrow compositional region in the BaO–TiO_2 phase diagram and a peritectoid decomposition temperature very close to that required for sintering. The attainment of the single phase needed to maintain good microwave dielectric properties demands exacting process control.

A series of "complex" perovskite compounds have been prepared, in which the B-sites of the lattice are shared by two ions of different valency [9]. These materials include $Ba(Zn_{1/3}Ta_{2/3})O_3$, $Ba(Zn_{1/3}Nb_{2/3})O_3$ and $Ba(Mg_{1/3}Ta_{2/3})O_3$, often referred to as BZT, BZN and BMT, respectively. Typical properties are $\varepsilon_r = 25$–30, $Q \approx 10\,000$ at 7 GHz and τ_f in the range $\pm 10\ \mathrm{MK}^{-1}$. These materials have excellent dielectric loss characteristics at higher frequencies ($f_0 > 10$ GHz), but their ε_r values are lower than those required for lower frequency applications ($f_0 \approx 1$ GHz).

Zirconium tin titanate (ZTS), a solid solution of ZrO_2, TiO_2 and SnO_2, or $Zr_xTi_ySn_zO_4$ where $x + y + z = 2$, offers perhaps the best compromise of properties and ease of processing for a wide range of applications. It has been the subject of a number of publications, reporting its structure, range of existence and dielectric properties [10]. The crystal structure [11] has been identified as being that of α-PbO_2, having orthorhombic symmetry and space group Pbcn. The Zr^{4+}, Ti^{4+} and Sn^{4+} ions are believed to be randomly distributed in the lattice each surrounded by slightly distorted oxygen octahedron.

The solid solution region of interest in the ZTS phase diagram is shown in Fig. 1. The relationship between electrical properties and composition is complex. However, in general it may be said that increasing the TiO_2 content at the expense of ZrO_2 or SnO_2 increases Q and ε_r, whilst increasing SnO_2 at the expense of ZrO_2 increases Q, but has little effect upon ε_r. Compositions with $\varepsilon_r = 35$, $Q = 10\,000$ and $\tau_f = \pm 2\ \mathrm{MK}^{-1}$ are readily identified.

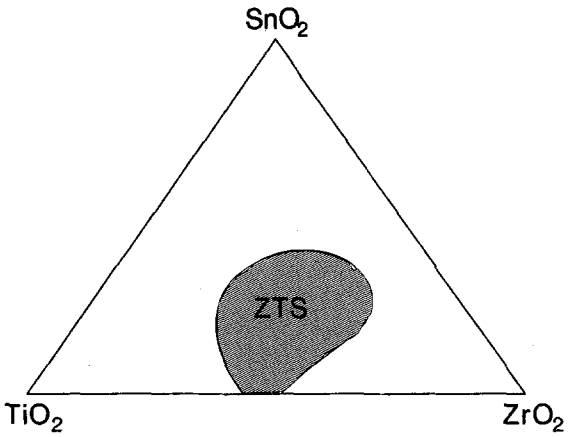

Figure 1 The extent of the solid-solution region in the ZTS equilibrium diagram.

It has been found that ZTS powders do not readily sinter by solid state diffusion, therefore sintering aids, such as ZnO, have been invariably added to achieve good densification at temperatures between 1200 and 1400°C. It is thought that these additives act by forming a liquid phase at the grain boundaries during sintering and so aid densification through rapid transport of matter through the liquid phase. There are a number of publications and patents which report upon the efficacy of a variety of sintering aids and dopants [10, 12, 13] which are employed to increase densification and enhance Q. These include ZnO, NiO, CuO, La_2O_3 and Fe_2O_3.

In the case of Fe_2O_3, deterioration in Q is caused by additions of approximately 0.5 wt %. However, it has been shown that this can be inhibited by the addition of NiO. Fe^{3+} is a common impurity in oxide ceramics and as a lattice defect might be expected to be distributed throughout the ZTS crystal structure. With the addition of NiO to the Fe-doped composition, an Fe–Ni spinel is formed at the grain boundaries, effectively removing the Fe^{3+} ions from the grain interiors. It is assumed that in the form of a grain boundary spinel the Fe^{3+} is less detrimental to the dielectric properties.

Although there is a satisfactory explanation for the influence of Fe_2O_3 and NiO upon the properties of ZTS, the behaviour of other additives is less well understood. In particular, the effect of ZnO, the most common sintering aid for this system, on the dielectric properties, is rather difficult to discern. Without a sintering aid, densities of > 90% theoretical have proved almost impossible to achieve by conventional routes and therefore microwave dielectric properties cannot be reliably related to those of a pure, dense ceramic. The presence of a grain-boundary phase due to the ZnO added to achieve adequate densities, may be assumed to cause significant deviations from the properties of a pure, dense material. Difficulties are therefore encountered in attempting to separate the intrinsic dielectric behaviour of ZTS from the influence of additives and microstructure.

The work reported herein was undertaken in an attempt to clarify the effects of the different types of additives and microstructural features on the microwave dielectric properties of zirconium tin titanate ceramics. The studies include the effects of liquid-phase sintering aids (e.g. ZnO), aliovalent dopants (e.g. La^{3+} and Nb^{5+}), porosity, grain-boundary phases, and grain size. An interpretation of the role of each of these in determining Q is attempted. An understanding of these effects is clearly of importance to the development of materials with higher Q values.

2. Experimental procedure

The materials studied were prepared by conventional solid state synthesis from the simple oxides of the cations of $> 99.5\%$ purity. A single ZrO_2–TiO_2–SnO_2 composition was used throughout, this being $Zr_{0.875}Ti_{0.875}Sn_{0.25}O_4$, subsequently referred to as ZTS. Additions of ZnO, La_2O_3 and Nb_2O_5 were made as detailed below.

The powders including additives were batched to the desired composition and placed in polypropylene bottles. They were milled for 16 h under propan-2-ol with zirconia milling media. The mixture was pan-dried in an oven at 60 °C and, when dry, passed through a 200 μm mesh nylon sieve before being calcined in open alumina crucibles at 1100 °C for 4 h. The calcined material was subsequently re-milled for 8 h under propan-2-ol with zirconia media. The resulting powder was dried and re-passed through the nylon sieve. All powders appeared to be single phase orthorhombic $(Zr, Ti, Sn)O_4$ when examined by X-ray powder diffraction (XRD) [14].

2.1. The effect of porosity on Q

To determine the influence of porosity on Q a method was devised to introduce small amounts of controlled porosity into the samples. Additions of small size polymethyl methacrylate (PMMA) spheres were made to ZTS powders. Two sizes of spheres, 4 μm and 90 μm, were used to discern the influence of pore size. A ZnO-modified material was used in order to avoid the effects of uncontrolled porosity that would be present in samples of "pure" ZTS. Thus, additions of the PMMA were made to a ZTS composition containing 1 wt% ZnO. The powder was dry mixed for 10 min in a three-dimensional turbula mixer, after which a 7 g pellet of diameter 12 mm was uniaxially pressed in a steel die at 55 MPa. Burn out of the spheres and sintering of the pellet were accomplished by following a ramp of 1 °C min^{-1}, with 2 h dwells at 200, 340, 600 and 1000 °C, with a final soak at 1350 °C for 4 h.

The densities of the sintered pellets were measured by the water immersion technique. The pellets were cut to size using a diamond saw and dried in an oven at 80 °C overnight in preparation for the measurement of microwave dielectric properties.

2.2. Sintering experiments

To study the effects of different additives and sintered grain size upon dielectric properties, three materials with different additives were fired for various times. The compositions studied were:

(A) ZTS + 1.0 wt % ZnO
(B) ZTS + 1.0 wt % ZnO + 0.5 wt % La_2O_3
(C) ZTS + 1.0 wt % ZnO + 0.5 wt % Nb_2O_5.

Pressed pellets of each composition were sintered in the range 1325–1375° C for up to 128 h. After firing, the weight loss, density, ε_r, Q, τ_f and grain size were all measured.

The grain-size measurements were made on polished sections etched in 60 vol % H_2SO_4 at 250 °C for 30 min. Micrographs were recorded using an optical microscope and 35 mm camera. Grain sizes were evaluated using the linear intercept method [15]. Approximately 1500 grains were counted for each sample, and a constant of 1.57 was used in the conversion from the average intercept length to grain size [16].

2.3. Dielectric property measurement

The dielectric properties of the specimens were measured by a dielectric post resonator technique, suggested by Hakki and Coleman [17] and Courtney [18]. In this method the relative permittivity and dielectric loss, or Q, are evaluated from the resonant frequency and width of a particular electromagnetic standing wave mode in a cylindrical sample of the dielectric. The analysis followed here is that of Hennings and Schnabel [19] with modifications to provide an absolute calibration of the system for loss measurements which does not rely on knowing the dielectric loss of a standard specimen.

A cylinder of the material to be characterized is placed between two parallel conducting plates to form a resonant cavity. Measurements are made in the transmission mode by coupling microwave power into and out of the cavity using two small antennae fashioned from the bared central conductor of semi-rigid microwave coaxial cable. The transmitted power as a function of frequency can be determined using a network analyser with a sweep oscillator as the source and is displayed as a ratio of the input power. At certain frequencies, which are functions of the dimensions and the relative permittivity of the resonator, resonance occurs, each frequency corresponding to a different electromagnetic mode. It is convenient to work with a low frequency, transverse electromagnetic mode, as the electric field goes to zero at the ends of the specimens which are in contact with the plates. This has the effect of minimizing losses due to conduction in the plates. Such modes are easily identifiable as, unlike other modes, there is minimal effect on their resonant frequency if one of the plates is slightly moved causing a small air gap between plate and specimen.

The particular mode chosen for these measurements is the H_{011}, sometimes known as the TE_{011} mode. Specimen sizes were chosen such that the resonant frequency of this mode fell within the range 4–6 GHz.

in which σ is the conductivity of the plates, μ_0 the permeability of free space and ε_0 the permittivity of free space. In practice this term is minimized by ensuring a high conductivity for the surface of the plates. This is achieved by electroplating with silver to a thickness greater than the skin depth at the measurement frequency and then polishing to a 1 μm finish.

The characteristic equation for the H_{011} mode is given by

$$\frac{\alpha J_0(\alpha)}{J_1(\alpha)} = -\frac{\beta K_0(\beta)}{K_1(\beta)} \quad (5)$$

with $J_v(x)$ and $K_v(x)$ being Bessel functions and modified Bessel functions, respectively, of the first kind and vth order, α is the radial wavenumber for radii less than that of the resonator, whilst β is the wave number for radii greater than the radius of the resonator. They are related by

$$\alpha^2 + \beta^2 = (\varepsilon_r - 1)(\pi D f_0/c)^2 \quad (6)$$

in which ε_r is the relative permittivity of the resonator, D the diameter, f_0 the resonant frequency and c the speed of light in a vacuum. Also

$$\beta = (\pi D f_0/c)[(c/2Lf_0)^2 - 1]^{1/2} \quad (7)$$

where L is the length of the resonator. If the resonant frequency of the TE_{011} mode is measured by the above method then the only unknown in the above three equations is ε_r. Finding ε_r necessitates solving the transcendental Equation 5. This can be done by numerical methods.

The width of the resonant peak is related to the Q or tan δ of the material. This is found by measuring the width of the peak, Δf, at 3 dB down from the maximum. The unloaded Q-factor, Q_0, is then given by

$$Q_0 = (f_0/\Delta f)/(1 - |S_{12}|) \quad (8)$$

The correction factor $1 - |S_{12}|$ can be kept close to 1 by weakly coupling the cavity. That is the resonant peak should be well below the reference level. Suitable insertion losses ($= 20\log|S_{12}|$) lie in the range -25 to -40 dB, so that the resonant peak is just above the noise limit. In practice this is achieved by increasing the separation of the antennae until the value of $f_0/\Delta f$ remains constant.

Hennings and Schnabel [19] have demonstrated that provided that the radius of the plates forming the cavity is sufficiently large, the most important contributions to Q_0 are from the losses in the specimen and from the conduction losses in the plates themselves. In practice the radius of the plates should be chosen to be approximately ten times that of the specimen. The dielectric loss of the specimen is then given by

$$\tan\delta = A/Q_0 - B \quad (9)$$

where A is a mode factor

$$A = 1 + FG/\varepsilon_r \quad (10)$$

with

$$F = J_1^2(\alpha)/[J_1^2(\alpha) - J_0(\alpha)J_2(\alpha)] \quad (11)$$

and

$$G = [K_0(\beta)K_2(\beta) - K_1^2(\beta)]/K_1^2(\beta) \quad (12)$$

Corrections for the plate conductivity are provided by the term B

$$B = (1 + FG)/[L^3(4\pi\sigma\mu_0^3\varepsilon_0^2\varepsilon_r^2 f_0^5)^{1/2}] \quad (13)$$

Equations 9–13 can be rearranged to give a relation of the form $y = mx + c$ in which $y = A/Q_0$, $c = \tan\delta$ and $m = \sigma^{-1/2}$. The only unknowns in this equation are tan δ, the loss of the specimen, and σ the conductivity of the plates. If several differently sized resonators of the same material are used, a plot of A/Q_0 against $(1 + FG)/[L^3(4\pi\mu_0^3\varepsilon_0^2\varepsilon_r^2 f_0^5)^{1/2}]$ will yield an intercept on the y-axis equal to tan δ and a slope equal to $\sigma^{-1/2}$.

To avoid possible inaccuracies due to variations of σ as a function of frequency, the resonators were chosen so that they were of approximately the same resonant frequency. Specimens with dimensions in the range $D/L = 0.6$–3.0 were used. As an approximate value for ε_r is usually known, it is a simple matter to calculate the dimensions of resonators for specific resonant frequencies in order to accomplish the tan δ measurements. Four specimens with dimensional ratios within the above range were usually sufficient to provide a straight line from which tan δ could be evaluated. From the regression analysis of this line errors on tan δ of less than $\pm$ 10% were typical. Reductions in this error can be achieved by using more than four specimens for each material.

In previously reported methods for the evaluation of tan δ, an independent measurement of σ or a standard dielectric specimen were required to correct for conduction losses in the plates. The above method does not require an assumed standard and provides an absolute measurement of the specimen tan δ. In practice, once a consistent value for σ has been established, the requirement for multiple specimens of each material can be relaxed. A mean derived value of σ can be inserted directly into the equations for single resonators.

The majority of measurements reported here were carried out for resonant frequencies of between 4 and 5.5 GHz. The Q values reported in the text have all been normalized to a measurement frequency of 4 GHz, assuming the empirical relationship $Q_0 f_0 =$ a constant.

3. Results

3.1. The effects of porosity on Q

The behaviour of the dielectric properties as a function of porosity was determined from those samples to which polymer spheres had been added. It was assumed that for densities of $< 98\%$ theoretical density (5.6 Mg m^{-3}) the deficit was totally due to porosity introduced from the burn-out of the PMMA spheres. ε_r and Q as a function of percentage of theoretical density, can be seen in Figs 2 and 3 respectively. ε_r is seen to decrease linearly with decreasing density, with only minor differences in behaviour being seen between those samples originally containing 4 or 90 μm spheres.

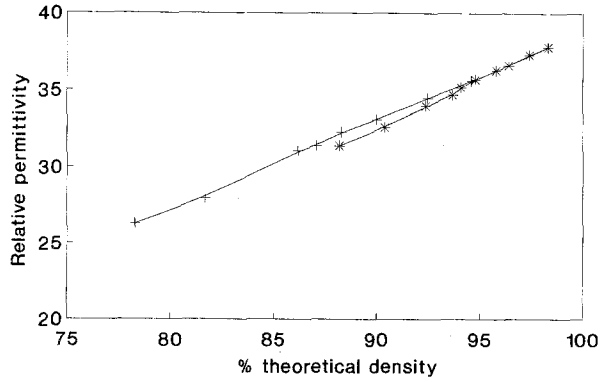

Figure 2 Relative permittivity as a function of percentage of theoretical density. (*) 4 μm PMMA spheres, (+) 90 μm PMMA spheres.

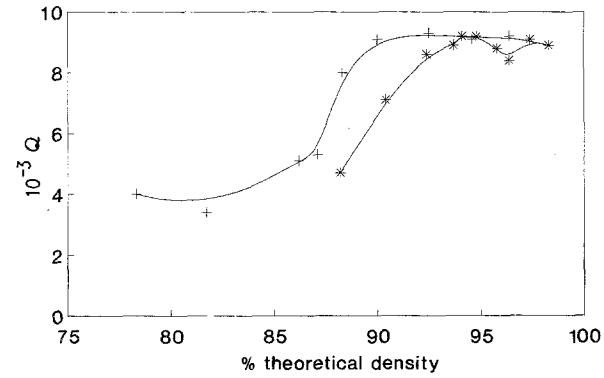

Figure 3 Q as a function of percentage of theoretical density. For key, see Fig. 2.

For materials of > 90% theoretical density, Q appears to be independent of porosity within the ± 10% accuracy limits of the measurement (Fig. 3). However, there is a marked decrease in Q with increasing porosity once the density has fallen below 90% theoretical.

3.2. Doping and the effects of sintering time

The influence of sintering time at 1350 °C on weight loss, sintered density, ε_r, Q and grain size for the compositions A to C can be seen in Figs 4–8. The behaviour reflected in these graphs is also typical of that seen at 1325 and 1375 °C. All samples underwent XRD analysis and no change, in either phase content

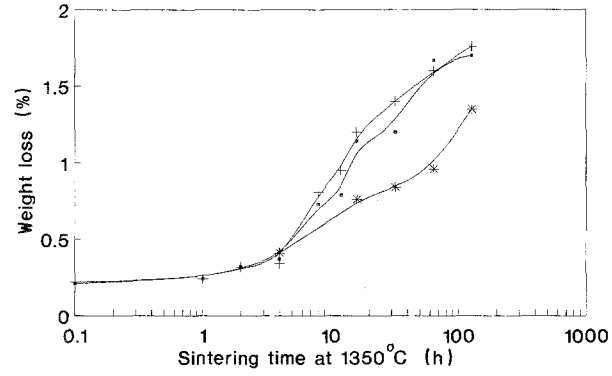

Figure 4 Weight loss as a function of sintering time at 1350 °C for compositions (■) A, (+) B, (*) C.

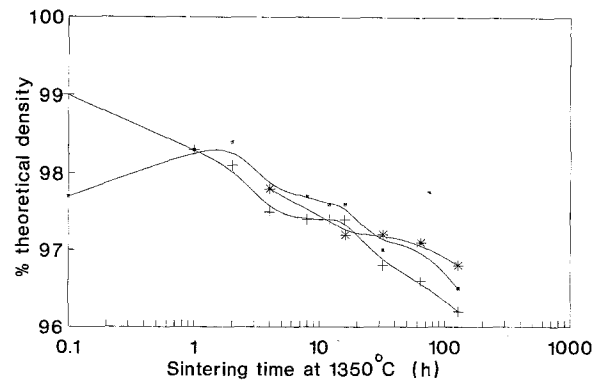

Figure 5 Percentage of theoretical density as a function of sintering time at 1350 °C. For key, see Fig. 4.

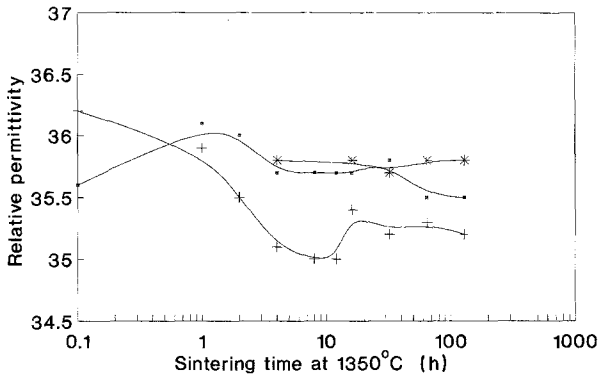

Figure 6 Relative permittivity as a function of sintering time at 1350 °C For key, see Fig. 4.

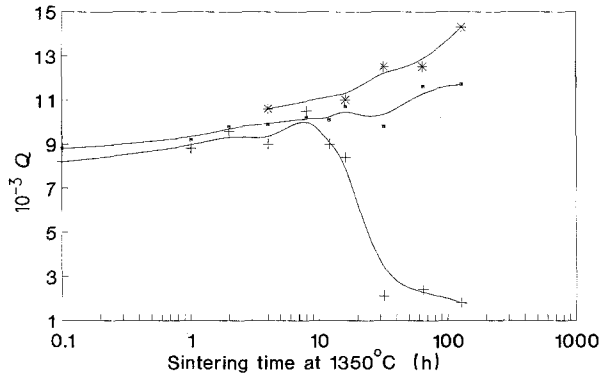

Figure 7 Q as a function of sintering time at 1350 °C. For key, see Fig. 4.

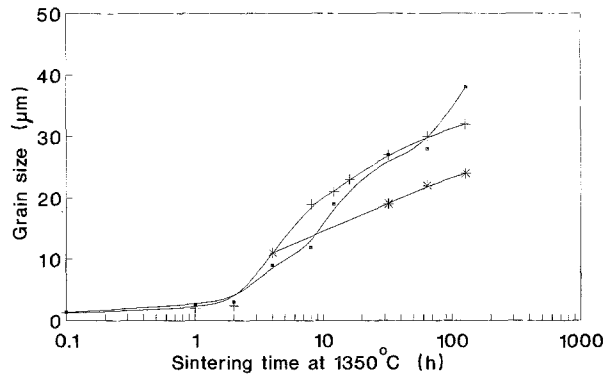

Figure 8 Grain size as a function of sintering time at 1350 °C. For key, see Fig. 4.

or lattice parameters, was detected with time or composition. Optical microscopy revealed no evidence for any second phases. However, ZnO-rich phases, not resolved by optical microscopy, presumed to exist at the grain boundaries, were confirmed during scanning and transmission electron microscopy using energy dispersive X-ray analysis. Fig. 4 illustrates that all samples lose mass as a function of sintering time. X-ray fluorescence (XRF) analyses of the cation composition demonstrate that ZnO is lost during sintering. For example, the ZnO content of composition A, sintered for 4 h at 1350 °C was 0.93 wt %. After 128 h this value was 0.10 wt %. As ZnO is the least refractory constituent of the compositions it is assumed that the loss occurs through volatilization. No change in the SnO_2 content was detected and other volatiles, such as water and organics picked up during the milling operation, are presumed to be responsible for the small weight losses that are apparent in addition to those of the ZnO.

The behaviour of ε_r as a function of sintering time is illustrated in Fig. 6. In all compositions there is a decrease in ε_r with increasing sintering time, which is consistent with the decrease in density (Fig. 5). Applying a density correction [20] to the permittivity data results in $\varepsilon_r = 37.1 \pm 0.3$ for all samples, independent of sintering time. The standard deviation is within the estimated measurement error of $\pm 1\%$. The temperature coefficient of resonant frequency (τ_f) was found to be independent of dopant type or sintering time and temperature, the value being $0 \pm 3\ MK^{-1}$ for all samples.

Q, as a function of sintering time, is shown in Fig. 7. Q of compositions A and C is seen to increase with time, in both cases, although the value for C, the Nb^{5+}-doped material, is consistently higher than that of A. However, Q of composition B (La^{3+}-doped) initially increases as a function of sintering time to a peak of 10 000, but after 10 h begins to decrease, until after 128 h at temperature it has a value of approximately 1000. This type of behaviour for composition B was also observed for specimens sintered at 1325 and 1375 °C. However, the sintering time after which Q starts to decrease is a function of temperature, being 16 and 8 h for sintering at 1325 and 1375 °C, respectively.

Microstructures of all samples show evidence of abnormal grain growth. After 4 h sintering there is evidence of pore entrapment in grains, and of a bimodal distribution of grain sizes. Further heat treatment results in grains with comparatively straight boundaries and a return to a more uniform grain size (Fig. 9a–c). Grain sizes as a function of sintering time are shown in Fig. 8. After 128 h at temperature, the La^{3+}-doped material (composition B) has twice the grain size of the Nb^{5+}-doped compositions (C).

Samples examined by scanning electron microscopy (SEM) revealed the presence of a second phase at the grain boundaries. Energy dispersive analysis of X-rays (EDAX) showed this to be a zinc–titanium compound, assumed to be in the form of Zn_2TiO_4. The presence of La^{3+} ions in the zinc titanate phase was confirmed for composition B, but Nb^{5+} ions were not found to be localized in the grain-boundary phase of composition C and were presumed to be evenly distributed throughout the matrix.

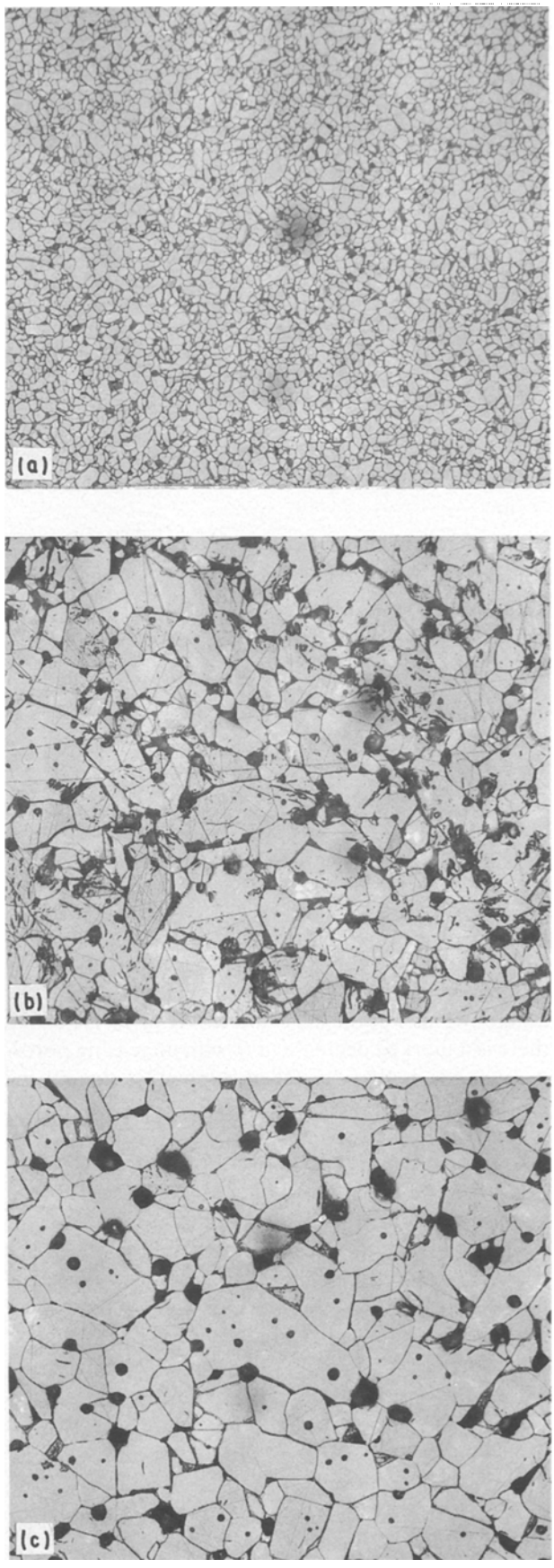

Figure 9 Optical micrographs of composition B after (a) 4 h, (b) 32 h and (c) 128 h at 1350 °C. × 200

4. Discussion

The nature of the relationship between density and Q is not readily explained. It is assumed that for materials of density $< 90\%$ theoretical, the decrease in Q, due to increasing porosity may be attributed to the effects of polarization at the pore surfaces. However, it might be expected that there should be some dependence upon pore size, with smaller pores producing a more marked degradation of Q. Although this appears to be the case, in this one experiment, the effect is perhaps not as marked as might be expected from a consideration of the pore surface areas. The fact that Q is virtually independent of porosity for densities greater than 90% theoretical, allows the effects of porosity to be neglected for most practical materials. The specimens considered in the remainder of this study were all of density greater than 95% theoretical and hence the influence of porosity on Q may be ignored.

Grain growth as a function of sintering time is a feature of all the compositions studied. As the behaviour of Q, expressed as a function of grain size, is markedly different for the three compositions, it may be assumed that grain size, *per se*, does not influence Q.

The improved densification of ZTS ceramics achieved through the addition of ZnO is attributed to a liquid-phase sintering mechanism, with the expectation that some liquid remains at the grain boundaries. This second phase, as shown by EDAX and transmission electron microscopy (TEM), is in the form of zinc titanate, Zn_2TiO_4. The dielectric properties of this composition have been measured by Wakino *et al.* [12] as $\varepsilon_r = 37$ and $\tan \delta > 0.1$ at 1 MHz. The presence of minor amounts of this phase at grain boundaries in ZTS is expected to lead to a reduction in Q of the ceramic, due simply to the additive effects of the introduction of an amount of a more lossy dielectric. Such a situation may be considered in terms of the known parallel and series mixing laws for dielectrics [21].

It has been shown that on prolonged sintering, ZnO volatilizes from the material, suggesting that the amount of second phase decreases as a function of sintering time. This explanation is consistent with the data shown in Fig. 7 for composition A, where Q increases with increasing sintering time. The volume of grain-boundary second phase is assumed to decrease and therefore contributes less to the measured dielectric properties. It can therefore be postulated that with increasing sintering time the composition of A approaches that of unmodified ZTS and Q may be assumed to approach the intrinsic value of the pure material. This is a significant result as it provides a rational estimate of the intrinsic dielectric properties of pure ZTS.

Interpretation of the results for compositions B and C requires consideration of the relative sizes of the dopant and principal cations. The La^{3+} ion is 30% larger than the largest of the principal cations, Zr^{4+}, and is unlikely to be accommodated as a substituent. The ZTS lattice does contain a number of large interstitial sites and La^{3+} ions may be assumed to be able to occupy these. However, during the initial stages of sintering, La^{3+} is considered to be located in the Zn–Ti–O grain-boundary phase.

In the case of composition B (La^{3+} doped), during sintering for prolonged periods, ZnO volatilizes from the sample and the composition of the grain boundary changes, leaving excess TiO_2 and La_2O_3 free to diffuse into the grains. The Ti^{4+} ions are assumed to take up their conventional sites in the lattice, whereas the La^{3+} ions enter as interstitials (using the notation of Kröger and Vink [22])

$$La_2O_3 \rightarrow 2La_i^{\cdot\cdot\cdot} + 3/2O_2 + 6e' \qquad (14)$$

Once the La^{3+} ions are present in the lattice they result in the formation of electrons as charge-compensating species. As an increasing mass of ZnO evaporates over longer sintering times, increasing numbers of La^{3+} ions become available to enter the lattice, resulting in a greater concentration of electrons. Although the band gap and conduction mechanism in ZTS have not been determined, it may be postulated that the increase in electron concentration results in an increase in the conductivity of the material, manifesting itself as a decrease in the dielectric Q at microwave frequencies. This hypothesis is consistent with the results of Fig. 7 for composition B. For short sintering times the ZnO losses produce a decrease in the volume of grain-boundary phase, without release of La^{3+} into the grains, which results in a slight increase in Q with increasing sintering time. However, after sintering for approximately 10 h, a quantity of ZnO has been lost such that all the La^{3+} cannot be accommodated by the grain-boundary phase. The excess La^{3+} ions migrate into the lattice resulting in a decrease in Q with increasing sintering time.

In contrast to La^{3+}, the Nb^{5+} ions are of similar ionic radius to the cations of the ZTS lattice and therefore may be assumed to have some solubility as substituents for either Zr^{4+}, Ti^{4+} or Sn^{4+}. EDAX investigations confirm that Nb^{5+} does not segregate to the grain boundaries and is therefore assumed to be present throughout the lattice. This distribution remains unaffected by changes in the composition of the grain-boundary phase as a function of sintering time. The observed changes in Q are therefore similar to those seen for composition A, in that Q increases due to the disappearance of the "lossy" grain-boundary phase. It is apparent, though, that the Q of the Nb-doped material is consistently higher than that of the undoped material (composition A). This may be explained by the possibility that Nb^{5+} ions are able to compensate for the effects of small quantities of common impurity ions, such as Fe_2O_3 and Al_2O_3, which may be present in the ZTS. These ions, which would act as acceptors, are present as impurities in the starting materials. The importance of small quantities of impurity acceptor ions has previously been acknowledged by Chan *et al.* [23] in the case of $BaTiO_3$. In ZTS, the impurities are thought to substitute on to the cation sites producing oxygen vacancies as lattice defects

$$Fe_2O_3 \rightarrow 2Fe'_{Zr} + 3O_O^x + V_O^{\cdot\cdot} \qquad (15)$$

The presence of Nb^{5+} ions is expected to reduce the

number of oxygen vacancies which result from the presence of impurities, minimizing the number of lattice defects

$$Nb_2O_5 \rightarrow 2Nb_{Zr}^{\cdot} + 4O_O^x + \tfrac{1}{2}O_2 + 2e' \quad (16)$$

$$Fe_2O_3 + Nb_2O_5 \rightarrow 2Fe_{Zr}' + 2Nb_{Zr}^{\cdot} + 8O_O^x \quad (17)$$

As discussed by Wakino *et al.* [24], the intrinsic microwave Q of this class of materials is a function of the lattice vibrational modes. Q may therefore be expected to vary as a consequence of changes to the material which influence the vibrational spectra. An example of this is the increase in Q of $Ba(Zn_{1/3}Ta_{2/3})O_3$ due to ordering of the lattice on volatilization of ZnO [25]. Similarly, other changes to the defect structure, such as a decrease in the oxygen vacancy concentration, might also be expected to produce an increase in Q, as demonstrated by the present work.

It can be seen from Equations 16 and 17 that increasing concentrations of Nb^{5+} ions will eventually lead to the introduction of electrons to the lattice. Indeed, it is observed that samples containing greater than 0.75 wt % Nb_2O_5 begin to change colour from cream to mid-grey to dark grey with increasing sintering time or dopant addition. The onset of the dark grey colouration corresponds to a decrease in Q, possibly associated with increased conductivity.

5. Conclusions

Evidence suggests that a number of loss mechanisms influence the Q of commercial ZrO_2–TiO_2–SnO_2 ceramic dielectrics used in microwave applications. Interfacial polarization is thought to play a role in porous materials, but for densities of greater than 90% theoretical there is no degradation of Q. Grain-boundary phases, due to the presence of ZnO as a sintering aid, reduce Q, again possibly due to the influence of interfacial polarization, but more probably through the parallel and series addition of a lossy dielectric. The role of the second phase is diminished as ZnO is volatilized during prolonged sintering. The effect of dopants depends upon their concentration and distribution between the bulk and grain-boundary phases. They may contribute electrons to the lattice resulting in a decrease in Q due to conductivity contributions, or may act to reduce lattice defects such as oxygen vacancies, thereby increasing Q through modification of the lattice vibrational modes.

References

1. J. K. PLOURDE and CHUNG-LI REN, *IEEE MTT* **29** (1981) 754.
2. R. D. RICHTMYER, *J. Appl. Phys.* **10** (1939) 391.
3. R. C. KELL, E. E. RICHES, P. BRIGGINSHAW and G. C. E. OLDS, *Elect. Lett.* **6** (1970) 614.
4. R. C. KELL, A. C. GREENHAM and G. C. E. OLDS, *J. Amer. Ceram. Soc.* **56** (1973) 352.
5. D. J. MASSE, R. A. PURCEL, D. W. READEY, E. A. MAGUIRE and C. P. HARTWIG, *Proc. IEEE* **59** (1971) 1628.
6. H. M. O'BRYAN, J. THOMSON and J. K. PLOURDE, *J. Amer. Ceram. Soc.* **57** (1974) 450.
7. H. M. O'BRYAN and J. THOMSON, *ibid.* **57** (1974) 522.
8. J. K. PLOURDE, D. F. LINN, H. M. O'BRYAN and J. THOMSON, *ibid.* **58** (1975) 418.
9. S. NOMURA, *Ferroelec.* **49** (1983) 61.
10. G. WOLFRAM and H. E. GOBEL, *Mater. Res. Bull.* **16** (1981) 1455.
11. R. E. NEWNHAM, *J. Amer. Ceram. Soc.* **50** (1967) 216.
12. K. WAKINO, K. MINAI and H. TAMURA, *ibid.* **67** (1984) 278.
13. US Pat. 4,785,375 TAM Ceramics, Inc. (1988).
14. JCPDS Reference Cards 34–31 to 34–33.
15. J. C. WURST and J. A. NELSON, *J. Amer. Ceram. Soc.* **55** (1972) 109.
16. M. I. MENDELSON, *ibid.* **52** (1969) 443.
17. B. W. HAKKI and P. D. COLEMAN, *IRE Trans. MTT* **8** (1960) 402.
18. W. E. COURTNEY, *IEEE Trans. MTT* **8** (1970) 476.
19. D. HENNINGS and P. SCHNABEL, *Philips J. Res.* **38** (1983) 295.
20. A. J. BOSMAN and E. E. HAVINGA, *Phys. Rev.* **129** (1963) 1593.
21. D. A. PAYNE and L. E. CROSS, in "Ceramic Microstructures", edited by R. M. Fulrath and J. A. Pask (Westview Press, Colorado, 1977) p. 548.
22. F. A. KRÖGER and H. J. VINK, in "Solid State Physics", Vol. 3, edited by F. SEITZ and D. TURNBULL (Academic Press, New York, 1981) p. 307.
23. N. H. CHAN, R. K. SHARMA and D. M. SMYTH, *J. Amer. Ceram. Soc.* **64** (1981) 556.
24. K. WAKINO, M. MURATA and H. TAMURA, *ibid.* **69** (1986) 34.
25. S. B. DESU and H. M. O'BRYAN, *ibid.* **68** (1985) 546.

Received 8 May
and accepted 16 May 1990